2343 BLS

Water Authority
of Western Australia

WATER RESOURCES DIRECTORATE

The Constant Head Well Permeameter Method

I. A Review Of Theoretical Advances

Report No. WH 37

May 1987

Water Authority
of Western Australia

WATER RESOURCES DIRECTORATE

Hydrology Branch

The Constant Head Well Permeameter Method

I. A Review Of Theoretical Advances

N J Schofield

Report No. WH 37

May 1987

Abstract

The constant head well permeameter is a commonly used method for measuring the in situ saturated hydraulic conductivity of soils above the water table. The method essentially involves drilling a well, filling it with water to a prescribed depth, maintaining a constant head of water in the hole, and measuring the inflow rate to the hole. Theories of water flow from a well in these conditions date back in excess of 25 years and some of the formulae derived for saturated hydraulic conductivity are still in use today. Recently several more sophisticated numerical and analytical studies have been reported. However a number of simplifying assumptions are still common to all analyses, including neglect of soil heterogeneity, macropore flow and air entrapment. In all but two of the most recent analyses, no account is taken of flow in mixed saturated-unsaturated conditions.

A review and comparison of the numerous formulae that have been developed to date have been carried out. In the analyses involving only saturated flow, the important variables in the formulae are head of water (h) and radius of well (a) which are conveniently expressed as the ratio $\gamma = h/a$. Comparison of saturated flow formulae over a range of γ revealed moderately good agreement. Solutions became in closer agreement at higher γ (>20) but were subject to increasing potential error at lower γ (<20).

Two analyses included mixed saturated-unsaturated flow from the well. The major conclusion from both analyses is that the predicted saturated hydraulic conductivity values are significantly less than for the assumption of saturated flow alone, due to the effect of capillarity. Also both formulae for saturated hydraulic conductivity involve an additional variable, α, the sorptive number, a quantity not easy to determine. The effect of capillarity is least for coarse soils and greatest for fine soils.

Saturated-unsaturated unsteady flow model analyses identified a number of characteristics useful to the design and operation of the constant head well permeameter. It was found that its efficiency of operation would be maximised by minimising the water/soil contact area, which requires a small well diameter and head of water. Two methods of terminating measurements prior to steady state infiltration being reached were suggested but these require further field evaluation.

CONTENTS

Figure Captions

Figure 1 Variables used in the analysis of flow out of a well above the water table (adapted from Reynolds et al., 1983)

Figure 2 Variables used in general pressure flow solution for a quadratic source-strength distribution (adapted from Reynolds et al., 1983)

Figure 3 Schematic representation of constant head permeameter in unsaturated soil showing the bulb of saturation

Figure 4 Comparison of K_s/Q solutions for a range of γ and $a = 0.01$ m, $\alpha = 1$ m^{-1}

Figure 5 Comparison of K_s/Q solutions for a range of γ and $a = 0.1$ m, $\alpha = 1$ m^{-1}

Figure 6 Variation of P3 and S-N solutions with a

Figure 7 Variation of P3 and S-N solutions with α

Figure 8 Infiltration rate as a function of time in GE3 silt loam for different borehole geometries (here r = borehole radius, A = length of borehole in contact with soil) (from Stephens and Neuman, 1982c)

Figure 9 Percentage of steady infiltration rate as a function of time for different borehole geometries in GE3 silt loam (here r = borehole radius, A = length of borehole in contact with soil) (from Stephens and Neuman, 1982c)

Tables

Table 1 Saturated hydraulic conductivity formulae

Table 2 ß values for four representative soils

Table 3 K_s/Q values for saturated hydraulic conductivity formulae for a range of γ and $a = 0.01$ m

Table 4 K_s/Q values for saturated hydraulic conductivity formulae for a range of γ and $a = 0.1$ m

Table 5 Volumes of water required to reach steady infiltration rates

1. Introduction

The measurement of the saturated hydraulic conductivity of soils has wide application in such areas as studies of streamflow generation and stream salinity, investigations of the spread of the root fungus (Phytophthora cinnamomi) resulting in jarrah dieback, phosphorus leaching from soils, and the siting of dams and irrigation canals.

Various methods have been developed to measure the in situ saturated hydraulic conductivity (permeability) of soils above the water table (in the unsaturated zone). These include ring or cylinder infiltrometer methods, the air entry permeameter method, the double tube method and various well permeameter methods. Constant head well permeameter methods can be broadly classified into open-end casing or open-hole types, both of which may be operated under gravity (water is allowed to infiltrate under gravity) or pressure (water is injected into the soil under pressure). When inflatable tubes are used to isolate intervals of a borehole, the tests are called packer tests and are usually conducted under pressure. The above methods have been described in several monographs including Boersma (1965), Bouwer and Jackson (1974) and USBR (1974, 1977).

The constant head well permeameter method is commonly used and essentially involves drilling a borehole, filling it with water to a prescribed depth, maintaining a constant head of water in the hole, and measuring the inflow rate to the hole. This apparently simple method has encountered a number of problems. The first of these relate to early designs where some of the difficulties included: an installation time of up to several hours; a measurement period of up to several days; a water requirement of up to 1000 L per measurement; and the need for at least two operators. The development of an in-hole Mariotte-type permeameter by Talsma and Hallam (1980) has alleviated these practical limitations. The authors claim that this permeameter is simply installed and can be operated by one person, requires only 0.5 - 2 L of water per measurement, and that measurements can often be made in 5 - 30 minutes.

The second set of problems with the constant head well permeameter method relates to the development of an appropriate theory. A number of formulae for calculating saturated hydraulic conductivity were derived more than 20 years

ago and are often still used. These were based on several simplifying assumptions, the most significant being the assumption of saturated flow away from the borehole in the presence of a free surface. More recently numerical solutions have been obtained, under the same assumptions, and have provided more accurate results by matching boundary conditions precisely (Stephens and Neuman, 1982a; Reynolds et al., 1983). However the major theoretical progress has resulted from the development of saturated-unsaturated flow models which take into account capillarity (Stephens and Neuman, 1982b; Philip, 1985a).

This report presents a review of theoretical developments.

2. Saturated Steady-State Flow Models

This section deals with analyses of flow out of a shallow well under the common assumptions of steady-state flow; a homogeneous, isotropic, rigid porous medium; and a semi-infinite, field-saturated flow domain.

2.1 General solution of flow out of a shallow well

Following Reynolds et al. (1983), the saturated hydraulic conductivity derived from flow out of a shallow well under the above assumptions is given by

$$K_s = \frac{C\,Q}{2\pi\,H^2\,(1 + 0.5\,C\,\gamma^{-2})} \qquad (1)$$

where Q is the outflow rate,

H is the constant height of water in the well above the base of the well,

$\gamma = H/a$

where a is the radius of the well

and

$$C = \left[-\int_0^1 \left. \frac{\partial \psi_p^*}{\partial r^*} \right|_{r^*=1} dz^* + \gamma^{-2} \int_0^1 \left. \frac{\partial \psi_p^*}{\partial z^*} \right|_{z^*=0} r^*\,dr^* \right]^{-1} \qquad (2)$$

where ψ_p is the pore water pressure head,

$$\psi_p^* = \psi_p / H,$$

r and z are the radial and vertical space variables (Fig. 1)

and $r^* = r/a$, $z^* = z/H$.

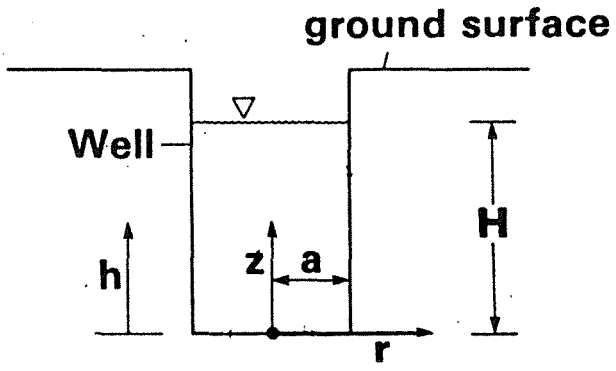

Figure 1 Variables used in the analysis of flow out of a well above the water table (adapted from Reynolds et al., 1983)

In situations where gravity flow is negligibly small compared with pressure flow, equation 1 simplifies to

$$K_s = \frac{C\,Q}{2\pi\,H^2} \qquad (3)$$

where Q represents pressure flow only.

It is clear that equation 2 must be evaluated in order to obtain K_s in equation 1 or 3. The radial pressure gradient $\partial\psi_p^*/\partial r^*$ and the vertical pressure gradient $\partial\psi_p^*/\partial z^*$ are, in general, functions of z^* and r^* respectively, for a given γ. The most commonly used approximate solutions are discussed briefly in the following.

2.2 Porchet solution

The Porchet solution neglects the functional nature of the pressure gradients in equation 2 and sets their dimensional forms, $\partial\psi_p/\partial r$ and $\partial\psi_p/\partial z$, to unity. Equation 2 then simplifies to

$$C = \left[\gamma^{-1} + 0.5\,\gamma^{-2}\right]^{-1} \qquad (4)$$

Setting the gradients to unity is equivalent to assuming that radial and vertical flow out of the well is due only to gravity and as such equation 4 can only be substituted into equation 3.

Both intuitive reasoning and predictions from pressure flow and numerical solutions (see below) suggest that pressure gradients are significantly greater than unity over much of their range. Consequently the Porchet approximation of unit gradient must significantly overestimate the true value of C.

2.3 General pressure flow solution for a quadratic source-strength distribution

Pressure flow solutions approximate the pressure gradients of equation 2 by gradients derived from various line sources with various source-strength distributions. The general pressure flow solution for quadratic source-strength distributions is described below and special cases of this, the Glover solution and the half-source solution follow in sections 2.4 and 2.5.

Steady-state pressure flow out of a well into a homogeneous, isotropic porous medium may be described in terms of the Laplace equation. The solution of the equation describes the pressure head distribution, ψ_p, about a point source of strength q, which in a symmetric, cyclindrical flow domain takes the form

$$\psi_p = \frac{q}{4\pi K_s}(r^2 + (z-h)^2)^{-1/2} \qquad (5)$$

where h is defined in Fig. 1

Steady flow out of the well can now be approximated by a continuous series of point sources of differing strengths arranged along the well axis. That is, the well and the steady flow from it, is, in effect, replaced by a line source of finite length and distributed strength. Various source locations along the axis of the well, and various source-strength distributions can be specified. In addition, line sinks can be coupled to the line sources, and different boundary conditions can be used.

A solution for a quadratic source-strength distribution is given below (see Reynolds et al. (1983) for derivation).

$$C = \frac{(1 - b^*)\,[\sinh^{-1}(\gamma\,(1-f^*)) - \sinh^{-1}(\gamma d^*)] - (\gamma^{-2} + (1-f^*)^2)^{1/2} + (\gamma^{-2} + d^{*2})^{1/2}}{2(1-b^*)\,[(1-b^*) - d^*] - 2(1-b^*)\,(1-f^*) + (1-f^*)^2 + d^{*2}} \quad (6)$$

where the constants b,d, and f determine the length and position of the source and sink as shown in Fig. 2, and the dimensionless variables b*, d* and f* are given by

$b^* = b/H$, $d^* = d/H$, $f^* = f/H$.

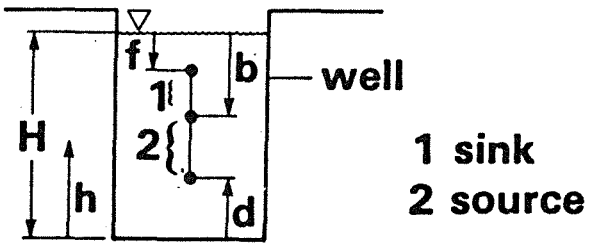

Figure 2 Variables used in general pressure flow solution for a quadratic source-strength distribution (adapted from Reynolds et al., 1983)

2.4 Glover solution

The Glover (1953) solution is a special case of the general solution for a quadratic source-strength distribution. In this case $b^* = d^* = f^* = 0$, which corresponds to a line source running from the bottom of the well to the water surface with no line sink. The Glover solution takes the form

$$C = \sinh^{-1}(\gamma) - (\gamma^{-2} + 1)^{1/2} + \gamma^{-1} \qquad (7)$$

When H >> a, equation (7) is often simplified to (Zangar, 1953)

$$C = \sinh^{-1}\gamma - 1 \qquad (8)$$

Because pressure flow and gravitational flow act independently of each other, equations 7 and 8 may be substituted into either equation 1 or equation 3. The original Glover solution only considered pressure flow and an obvious improvement is to substitute equation 7 into equation 1 and thereby include gravity flow.

2.5 Nasberg - Terletskaya solution

Nasberg (1951) developed a formula for K_s based on an approach similar to that of Glover (1953), except that he included an image point sink to satisfy more closely the free surface boundary condition and to account for the presence of a stagnation point above the point source. Terletskaya (1954) extended Nasberg's work to the case of a line source by integrating Nasberg's point source solution along the well, treating the strength of the source as a constant. Terletskaya extended her solution to approximate a cylindrical source by imposing a prescribed pressure head at the bottom of the borehole along its radius, in a manner similar to that of Glover. The Nasberg-Terletskaya formula takes the form

$$K_s = \frac{Q \log(2\gamma)}{2.364\, H^2} \qquad (9)$$

and is applicable in the range $50 < \gamma < 200$.

2.6 Reynolds, Elrick and Topp half-source solution

An alternative special case of the general solution for a quadratic source-strength distribution was found by Reynolds et al. (1983) to be more accurate than the Glover solution for γ values between 5 and 10. This solution, termed the half-source solution, has $b^* = f^* = 0.5$, and $d^* = 0$, which corresponds to a line source extending from the bottom of the well to half-way to the water surface with no line sink. The C value takes the form

$$C = 4\left[0.5\ \sinh^{-1}\ (0.5\ \gamma) - (\gamma^{-2} + 0.25\ )^{1/2} + \gamma^{-1}\right] \qquad (10)$$

The half-source C values may be substituted into either equation 1 or equation 3.

2.7 Reynolds, Elrick and Topp numerical solution

A numerical solution for the pressure gradients in equation 2 was obtained by Reynolds et al. (1983) for the steady-state pressure head distribution in a cylindrical flow domain surrounding the well. This approach has the advantage of matching the pressure head distributions along the wall and base of the well exactly, whereas the previous approximate analytical solutions do not.

Pressure flow in a cylindrically symmetric flow domain may be described by the cylindrical, non-dimensional Laplace equation

$$\frac{1}{r^*}\ \gamma^2\ \frac{\partial}{\partial r^*}\ \left(r^*\ \frac{\partial \psi_p^*}{\partial r^*}\right)\ +\ \frac{\partial}{\partial z^*}\left(\ \frac{\partial \psi_p^*}{\partial z^*}\right)\ =\ 0 \qquad (11)$$

Equation 11 was converted into its five point central finite difference analogue and solved, subject to specified boundary conditions. Once the pressure head distribution in the flow domain was obtained, the pressure head gradients along the wall and base of the well were estimated.

2.8 Stephens and Neuman numerical solution

Stephens and Neuman (1982b) evaluated the accuracy of some of the analytical formulae using a finite element model of free surface flow developed by Neuman and Witherspoon (1970). This model guarantees that all of the boundary conditions are properly satisfied, which is not the case with the analytical solutions. The finite element computer program is entitled FREESURF for which Neuman (1976) has published a User's Guide. Details of the mathematical formulation of the free surface problem for borehole infiltration tests can be found in Stephens and Neuman (1982a).

Comparison of FREESURF to the Glover solution over the range $10 < \gamma < 1000$, showed significant differences for $\gamma > 50$ but close agreement for $\gamma \sim 10$. The opposite occurred with comparison to the Nasberg-Terletskaya solution, where reasonable agreement with FREESURF solution was found for $\gamma > 50$ but significant differences for $\gamma < 30$. Stephens and Neuman (1982b) did not provide an empirical formula for this problem. Reference should be made to their paper for further details.

2.9 Philip analytic solution

Philip's (1985a) analysis of the steady constant-head uncased borehole permeameter involved deriving an approximate solution to saturated flow within a bulb-shaped region located adjacent to, and extending below the borehole (Stephens and Neuman, 1982b), as shown in Fig. 3. Within the saturated bulb, steady flow in a homogeneous isotropic medium was described by:

$$\nabla^2 \Phi = 0 \tag{12}$$

where Φ is the total potential. The solution to equation 12, subject to appropriate boundary conditions, was found by combining a solution given by Philip (1985b) with one given by Carlsaw and Jaeger (1959). Re-arrangement of Philip's (1985a) solution yields

$$K_s = \frac{Q\,(\ln [\gamma + (\gamma^2 - 1)^{1/2}] - (1 - \gamma^{-2})^{1/2})}{4.117\, a^2\, \gamma\, (\gamma^2 - 1)^{1/2}\, (1 - \gamma^{-2})} \tag{13}$$

which, for the case $\gamma >> 1$, simplifies to

$$K_s = \frac{Q\,[\ln (2\gamma) - 1]}{4.117\, a^2\, \gamma^2} \tag{14}$$

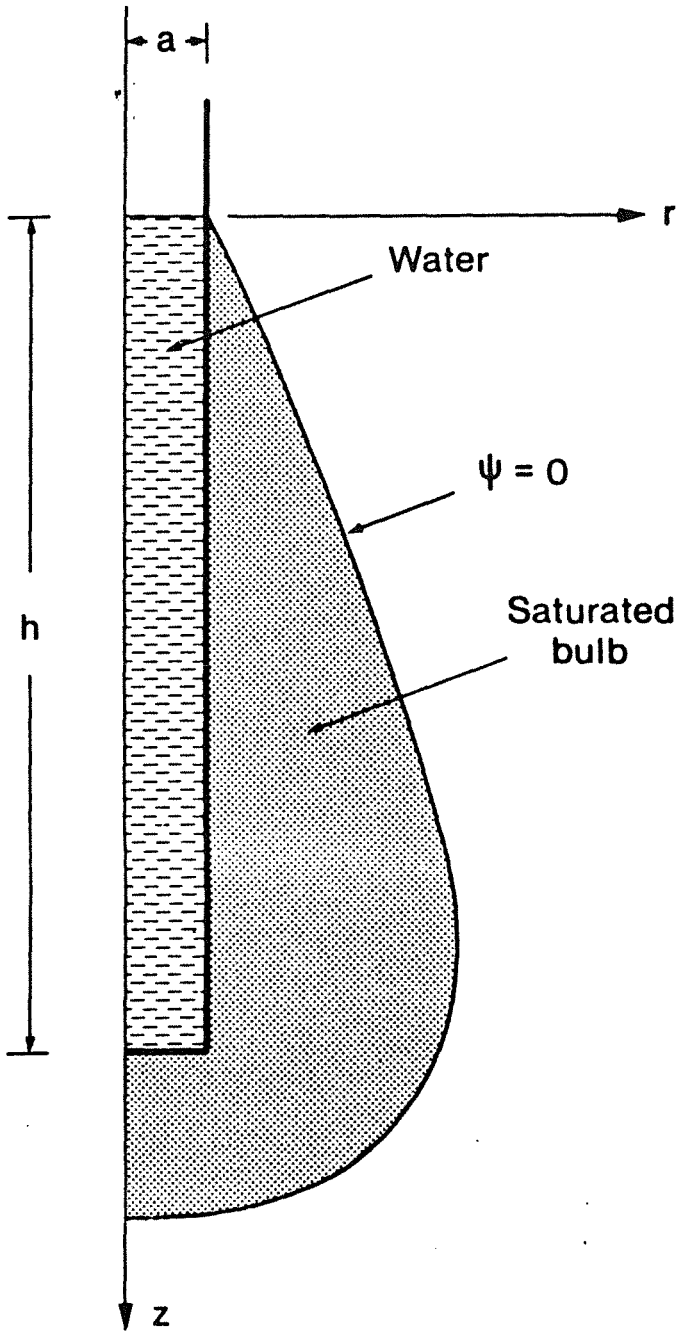

Fig. 3 Schematic representation of constant head permeameter in unsaturated soil showing the bulb of saturation

3. Saturated-Unsaturated Steady-State Flow Models

All the solutions described in Section 2 were based on the approximation of saturated flow in the presence of a free surface. However, as Philip (1966, 1969) pointed out, the steady 3-dimensional flow of free water from any soil surface of finite area into a surrounding unsaturated soil depends not only on the saturated hydraulic conductivity of the soil, but also on the capillary absorptive properties of the soil. The magnitude of this capillarity effect has been shown to be highly significant.

3.1 Stephens and Neuman numerical solution

Stephens and Neuman (1982b) employed two numerical models capable of handling saturated-unsaturated soil water movement. Both were single-phase water flow models which did not account for air entrapment. One of the models, entitled FLUMP, was based on a mixed explicit-implicit finite element scheme developed by Neuman and Narasimhan (1977) and described in Narasimhan et al. (1978). The second flow model, TRUST, was based on an integrated finite difference approach in conjunction with a similar mixed explicit-implicit iterative method. Details of this scheme can be found in Narasimhan and Witherspoon (1977). Both models produced nearly identical results for the axisymmetric, steady-state case, although TRUST required less computer time.

The models were applied to infiltration from an open borehole in four soils representing the range of soil hydraulic properties. The soils were selected from a compendium of unsaturated soil hydraulic properties, catalogued according to soil texture, and published by Mualem (1976). The selected soils were Yolo light clay, G.E.3 silt loam, Del Monte find sand and a hypothetical coarse sand with properties similar to No. 4107 in Maulem's catalogue. The results showed that the calculated saturated hydraulic conductivity is strongly dependent on soil type. Comparison to the Glover solution showed that the Glover solution predicted generally, though not always, significantly higher K_s values. In the case of a silt loam, Glover's formula exceeded the numerical solution value by 50-60%, whereas in the case of a coarse sand, the Glover formula slightly underestimated K_s.

Comparison of the saturated-unsaturated analysis to the FREESURF model indicated that a significant portion of the total flow took place outside the region defined by the classical free surface envelope. In general the degree to which streamlines diverged increased with the water retention capacity of the soil.

Based on the results of testing the effect of varying H and a, for the range of representative soils, the authors were able to develop an empirical regression formula for K_s, which upon re-arrangement takes the form

$$\log K_s = \log \frac{Q}{aH} - 0.658 \log \gamma + 0.238 \beta^{1/2} + 0.398 \log H - 1.343 \qquad (15)$$

where β is a parameter representing the average slope of $\ln K_r$ versus ψ over the range $0.5 < K_r < 1$, defined as

$$\beta = \ln 0.5/\psi(K_r = 0.5) \qquad (16)$$

where K_r is the relative hydraulic conductivity defined as

$$K_r = K(\psi)/K_s \quad .$$

In equation 15, H is in metres and β is in inverse metres.

3.2 Philip analytic solution

Philip (1985a) carried out a saturated-unsaturated flow analysis in which an approximate model of saturated flow inside a saturated bulb forming adjacent to and below the well was matched to an approximate model of unsaturated flow outside the bulb. The total potential gradient inside the bulb exceeds that due to gravity because of capillarity effects operating outside the bulb. The capillarity potential was modelled by $-2D\,\alpha^{-1}$, where D is a numerical coefficient and α is the 'sorptive number' defined below. D was obtained by matching flow distributions inside and outside the saturated bulb.
Unsaturated flow was treated by an approximate quasi-linear analysis in which the bulb surface was replaced by a spheroidal surface. The outcome was that D had a mild dependence on γ, which took the form

$$D = 0.56 + 0.35\,\gamma^{-1} \qquad 2 < H < 200 \qquad (17)$$

The full solution for saturated hydraulic conductivity, obtained by re-arranging the Philip's (1985a) equation 32, is

$$K_s = Q(\gamma^2-1)^{-1/2}\left[\frac{4.117\ aH\ (1-\gamma^{-2})}{\ln\left[\gamma + (\gamma^2-1)^{1/2}\right] - (1-\gamma^{-2})^{1/2}} + \frac{4.028a + 2.517a\ \gamma^{-1}}{0.5\ \alpha\ \ln\left[\gamma + (\gamma^2-1)^{1/2}\right]}\right]^{-1} \qquad (18)$$

where the parameter α, the 'sorptive number', is a measure of the capillary properties of a soil defined in the relationship

$$K(\psi) = K_s\ e^{\alpha\psi} \qquad \alpha > 0,\ \psi < 0 \qquad (19)$$

α typically ranges from 0.2 m^{-1} for fine soils to 5 m^{-1} for coarse soils.

For the case $\gamma >> 1$, equation 18 reduces to:

$$K_s = \frac{Q}{aH}\left[\frac{4.117\ \gamma}{\ln\ (2\gamma)-1} + \frac{4.028}{0.5\ \alpha\ a\ \ln(2\gamma)}\right]^{-1}$$

3.3 Comparison of saturated hydraulic conductivity formulae

The saturated hydraulic conductivity formulae derived in the previous sections are listed in Table 1 and are annotated by a symbol for easy reference.

Table 1 Saturated hydraulic conductivity formulae

Author	Section	Equation	Notation
Porchet	2.2	$K_s/Q = C/(2\pi a^2\ \gamma^2)$ where $C = (\gamma^{-1}+0.5\ \gamma^{-2})^{-1}$	P
Glover	2.4	$K_s/Q = C/[2\pi a^2\ \gamma^2(1+0.5\ C\ \gamma^{-2})]$ where $C = \sinh^{-1}(\gamma)-(\gamma^{-2}+1)^{1/2}+\gamma^{-1}$	G1
Glover	2.4	$K_s/Q = C/(2\pi a^2\ \gamma^2)$ where $C = \sinh^{-1}(\gamma)-(\gamma^{-2}+1)^{1/2}+\gamma^{-1}$	G2
Zangar	2.4	$K_s/Q = C/[2\pi a^2\ \gamma^2(1+0.5\ C\ \gamma^{-2})]$ where $C = \sinh^{-1}(\gamma)-1$	Z1

Zangar	2.4	$K_s/Q = C/(2\pi a^2\gamma^2)$ where $C = \sinh^{-1}(\gamma)-1$	Z2
Reynolds et al.	2.6	$K_s/Q = C/[2\pi a^2\ \gamma^2(1+0.5\ C\ \gamma^{-2})]$ where $C = 4\ [0.5\ \sinh^{-1}(0.5\ \gamma)-(\gamma^{-2}+0.25)^{1/2}+\gamma^{-1}]$	R1
Reynolds et al.	2.6	$K_s/Q = C/(2\pi a^2\ \gamma^2)$ where $C = 4[0.5\ \sinh^{-1}(0.5\ \gamma)-(\gamma^{-2}+0.25)^{1/2}+\gamma^{-1}]$	R2
Reynolds et al.	2.7	$K_s/Q = C/[2\pi a^2\ \gamma^2\ (1+0.5\ C\ \gamma^{-2})]$ where $C = 2.2$ for $\gamma = 5$, $C = 3.3$ for $\gamma = 10$	R3
Reynolds et al.	2.7	$K_s/Q = C/(2\pi a^2\ \gamma^2)$ where $C = 2.2$ for $\gamma = 5$, $C = 3.3$ for $\gamma = 10$	R4
Nasberg-Terletskaya	2.5	$K_s/Q = \log\ (2\gamma)/(2.364\ a^2\gamma^2)$	N-T
Philip	2.9	$\frac{K_s}{Q} = \frac{\ln[\gamma+(\gamma^2-1)^{1/2}]+(1-\gamma^{-2})^{1/2}}{4.117\ a^2\ \gamma\ (\gamma^2-1)^{1/2}(1-\gamma^{-2})}$	P1
Philip	2.9	$K_s/Q = [\ln(2\gamma)-1]/(4.117a^2\ \gamma^2)$	P2
Philip	3.2	$\frac{K_s}{Q} = (\gamma^2-1)^{-1/2}\left[\frac{(4.117\ a^2\ \gamma(1-\gamma^{-2})}{\ln\ [\gamma+(\gamma^2-1)^{1/2}]\ -\ (1-\gamma^{-2})^{1/2}}\right.$ $\left. +\ \frac{4.0275a\ +\ 2.517a\ \gamma^{-1}}{0.5\ \alpha\ \ln[\gamma+(\gamma^2-1)^{1/2}]}\right]^{-1}$	P3
Philip	3.2	$\frac{K_s}{Q} = \frac{1}{a^2\gamma}\left[\frac{4.117\ \gamma\ +}{\ln\ (2\gamma)-1}\ \frac{4.028}{0.5\ \alpha\ a\ \ln(2\gamma)}\right]^{-1}$	P4
Stephens & Neuman	3.1	$\log\ \frac{K_s}{Q} = \log\ \frac{1}{a^2\gamma} - 0.658\ \log\ \gamma + 0.238\ \beta^{1/2}$ $+ 0.398\ \log\ a\gamma - 1.343$	S-N

Two additional variables appear in equations P3, P4 and S-N, namely α and β. α is defined by the relation:

$$K(\psi) = K_s\ e^{\alpha\psi}$$

or $$\ln K_r = \alpha\psi \qquad (20)$$

β is defined as the slope of the $\ln K_r - \psi$ relation over the range $0.5 < K_r < 1$. Assuming that this definition of slope is also suitable for α, then α and β may be regarded as interchangeable. Stephens and Neuman (1982b) presented $K_r - \psi$ graphs for four soils representing a wide range of soil textures from which β values have been extracted (Table 2).

Table 2 ß values for four representative soils

Soil	K_s (md^{-1})	$\psi(K_r = 0.5)$ (m)	ß (m^{-1})
coarse sand	40	0.14	5.1
fine sand	0.38	0.54	1.3
silt loam	0.05	0.68	1.0
light clay	0.01	0.16	4.3

The ß values for these soils (Table 2) cover the range 1 - 5 m^{-1}, whereas Philip (1985a) suggests that α varies from 0.2 - 5 m^{-1}, the upper limit corresponding to coarse sand.

Comparison of equations

The major solutions of Table 1 have been compared by plotting log K_s/Q v γ for a = 0.01 m, α = 1 m^{-1} as shown in Fig. 4. Several observations are made in the following.

(i) It is clear that the Porchet solution predicts significantly greater K_s/Q values than the other solutions. Due to the limitations of the approximations used in its derivation, it should be eliminated from further consideration.

(ii) The saturated flow solutions of Reynolds et al. (R2), Nasberg - Terletskaya (N-T), Glover (G1) and Philip (P2) agree fairly well, with the Glover solution diverging most from this group.

(iii) The saturated-unsaturated flow solutions of Philip (P3) and Stephens-Neuman (S-N) predict significantly smaller K_s/Q values than the saturated flow solutions for the whole range of γ at a = 0.01 m, α = 1 m^{-1}.

(iv) The P3 and S-N solutions agree well at γ>50 but increasingly less well as γ decreases from 50, for a = 0.01 m, α = 1 m^{-1}.

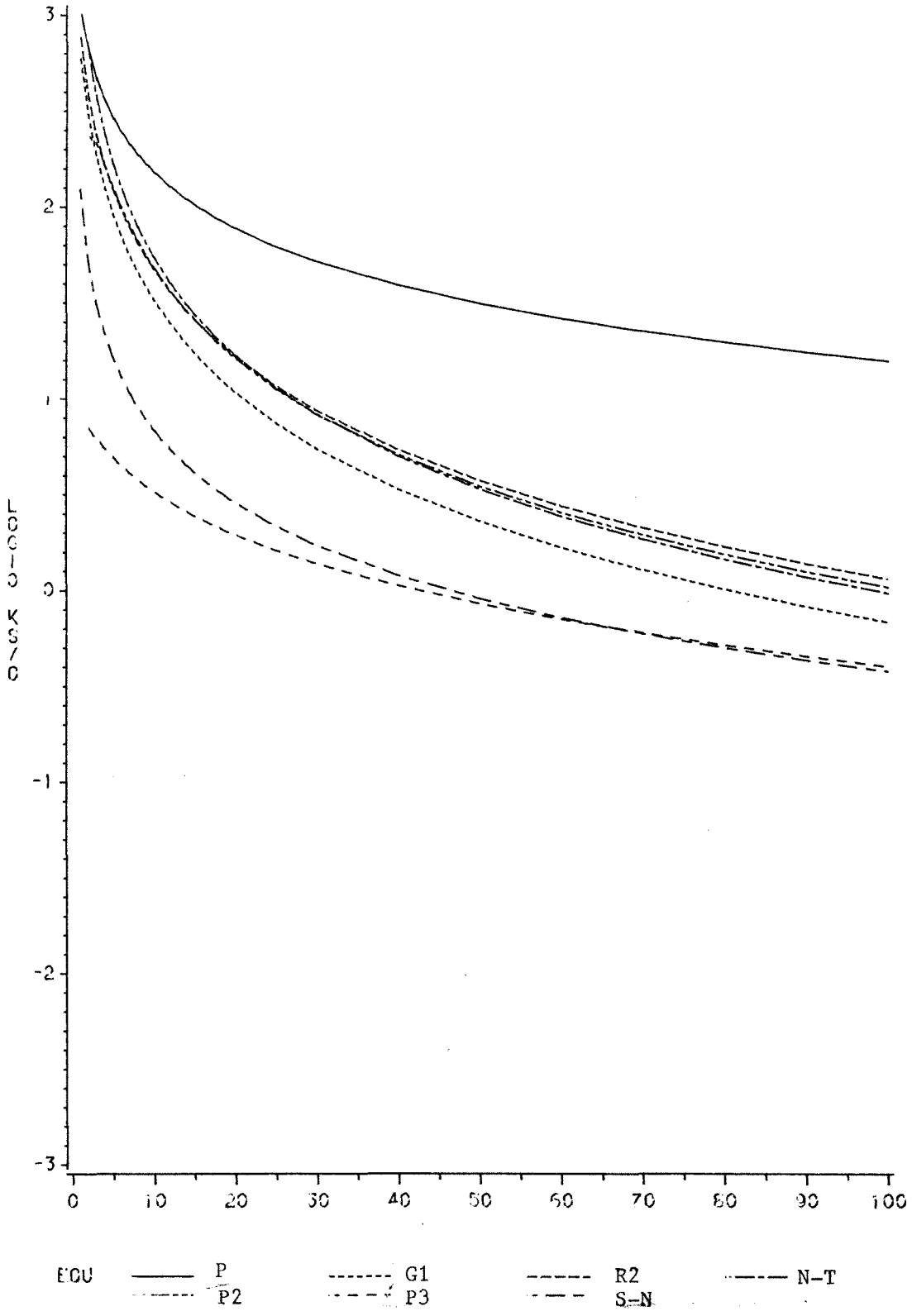

Figure 4 Comparison of K_s/Q solutions for a range of γ and a = 0.01 m, $\alpha = 1m^{-1}$

(v) All the solutions tend towards low log-linear gradients at $\gamma>20$ but at $\gamma<20$ the gradients become very high, indicating that small errors in the measurement of γ would give large errors in K_s/Q.

(vi) Excluding the Porchet solution, the bandwidth of solutions for K_s/Q tends to decrease with increasing γ.

Fig. 5 shows the same equations plotted as Fig. 4 but with a = 0.1 m. This change in a is seen to significantly reduce the bandwidth of solutions for K_s/Q (excluding the Porchet solution). As before the R2, N-T and P2 solutions agree well and the G1 solution diverges at higher γ. In this example the P3 and S-N solutions approach the saturated solutions (except G1) at high γ.

Comparison of solutions for general equations 1 and 3 and approximate solutions at $\gamma>>1$

Numerical values of the full set of equations in Table 1 are given in Table 3 (a = 0.01 m) and Table 4 (a = 0.1 m) for a range of γ. In general there was very little difference between the solutions using either equation 1 or equation 3. For solutions approximated for $\gamma>>1$, there was very close agreement to their unapproximated forms for $\gamma>20$.

The effects of 'a' and α on the saturated-unsaturated flow equations

It is clear from Figs. 4 and 5 and Tables 3 and 4 that both 'a' and α have a significant impact on predicted K_s/Q values of the P3 and S-N solutions. The impact of 'a' on the P3 and S-N solutions is shown more clearly in the log-log plots of Fig. 6. In this figure the S-N solution is linear and the P3 solution near linear and of similar gradient. Over the normal range of 'a' values used it is clear that the P3 and S-N solutions will not differ greatly. In both cases, an order of magnitude change in 'a' results in a slightly greater than order of magnitude change in K_s/Q.

The variation of the P3 and S-N solutions with respect to α is shown in the log-log plots of Fig. 7. In this case the solutions are clearly non-linear (on log-log scales) and of inverse curvature. It is clear that the two

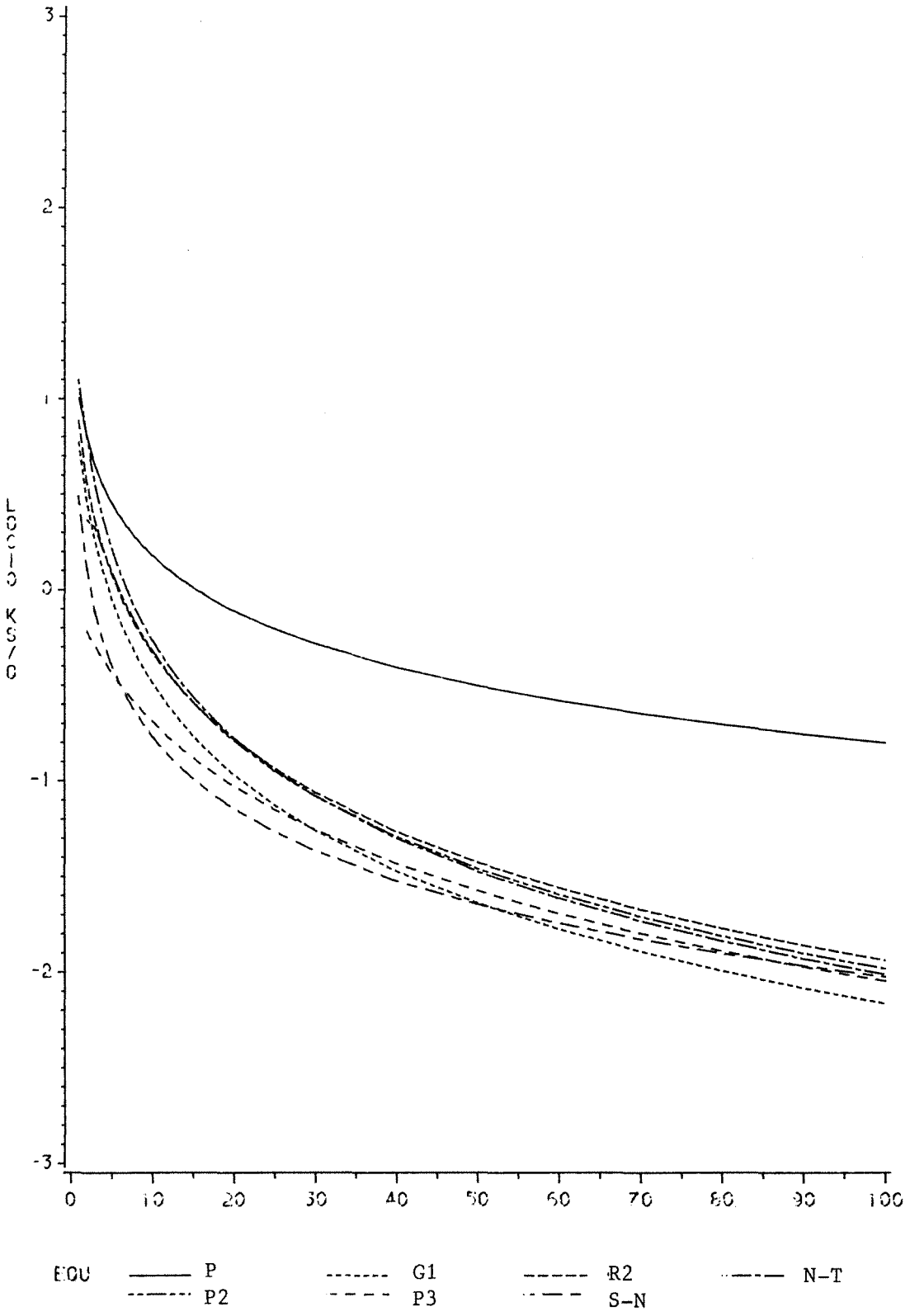

Figure 5 Comparison of K_s/Q solutions for a range of γ and a = 0.1 m, $\alpha = 1\ m^{-1}$

Table 3 K_s/Q values for saturated hydraulic conductivity formulae for a range of γ and a = 0.01 m

	γ				
	5	10	20	50	100
P	289.5	151.6	77.7	31.5	15.8
G1	92.3	33.0	10.9	2.31	0.69
G2	95.1	33.3	10.9	2.31	0.69
Z1	81.5	31.5	10.7	2.29	0.68
Z2	83.6	31.8	10.7	2.30	0.68
R1	119.0	46.8	16.6	3.75	1.15
R2	123.6	47.5	16.7	3.76	1.15
R3	134.2	51.7	-	-	-
R4	140.1	52.5	-	-	-
N-T	169.2	55.0	16.9	3.38	0.97
P1	135.6	49.3	16.4	3.51	1.04
P2	126.6	48.5	16.3	3.50	1.04
P3 (α = 0.2)	1.02	0.69	0.43	0.21	0.116
P3 (α = 1)	4.97	3.28	1.96	0.85	0.40
P3 (α = 5)	21.7	13.0	6.62	2.16	0.79
P3 (α = ∞)	135.6	49.3	16.34	3.50	1.04
P4 (α = 0.2)	1.13	0.73	0.45	0.21	0.12
P4 (α = 1)	5.47	3.45	2.01	0.86	0.40
P4 (α = 5)	23.3	13.4	6.73	2.17	0.79
S-N (β = 0.2)	12.2	5.10	2.13	0.67	0.28
S-N (β = 1)	16.5	6.90	2.88	0.91	0.38
S-N (β=5)	32.5	13.6	5.67	1.79	0.75

solutions will only agree well at or near the two points of intersection of the curves (α ~ 0.8, 7 in this case). The lower gradients of the two curves for α in comparison to 'a', indicates that K_s/Q predicted values are more tolerant to changes in α. However greater errors and uncertainty are normally associated with the measurement of α.

The effect of capillarity in the P3 solution is evident from Tables 3 and 4 where values of K_s/Q for a range of α and γ are listed. The value of $\alpha = \infty$ corresponds to zero capillarity. It is clear that the effect of capillarity on K_s/Q values is greater for finer soils (α decreasing).

Table 4 K_s/Q values for saturated hydraulic conductivity formulae for a range of γ and a = 0.1 m

	γ				
	5	10	20	50	100
P	2.90	1.52	0.78	0.32	0.19
G1	0.92	0.33	0.11	0.023	0.007
G2	0.95	0.33	0.11	0.023	0.007
Z1	0.81	0.32	0.11	0.023	0.007
Z2	0.84	0.32	0.11	0.023	0.007
R1	1.19	0.47	0.17	0.038	0.012
R2	1.24	0.48	0.17	0.038	0.012
R3	1.34	0.52	-	-	-
R4	1.40	0.53	-	-	-
N-T	1.69	0.55	0.17	0.034	0.010
P1	1.36	0.49	0.16	0.035	0.010
P2	1.27	0.48	0.16	0.035	0.010
P3 (α = 0.2)	0.096	0.062	0.035	0.014	0.006
P3 (α = 1)	0.37	0.21	0.094	0.027	0.009
P3 (α = 5)	0.89	0.38	0.14	0.033	0.010
P3 (α = ∞)	1.36	0.49	0.16	0.035	0.010
P4 (α = 0.2)	0.105	0.064	0.036	0.014	0.006
P4 (α = 1)	0.39	0.21	0.095	0.027	0.009
P4 (α = 5)	0.88	0.38	0.14	0.033	0.010
S-N (β = 0.2)	0.31	0.13	0.053	0.017	0.007
S-N (β = 1)	0.41	0.17	0.072	0.023	0.009
S-N (β=5)	0.81	0.34	0.14	0.045	0.019

However the effect of capillarity decreases as H increases (i.e. as γ increases with 'a' constant) and as 'a' increases (compare Table 4 to Table 3). Thus it appears that in practical applications the effect of capillarity can be reduced or in some cases neglected by using larger boreholes and greater heads of water. This however would not generally be a practical option without artificially pressurising the water column to increase the head. Thus the use of P3 is generally reliant on a measurement of α.

The effect of capillarity in the S-N solution is evident from Tables 3 and 4 and Fig. 7 but is not nearly as strong as the P3 solution. In this case there is no significant change in capillarity effect with H or 'a'.

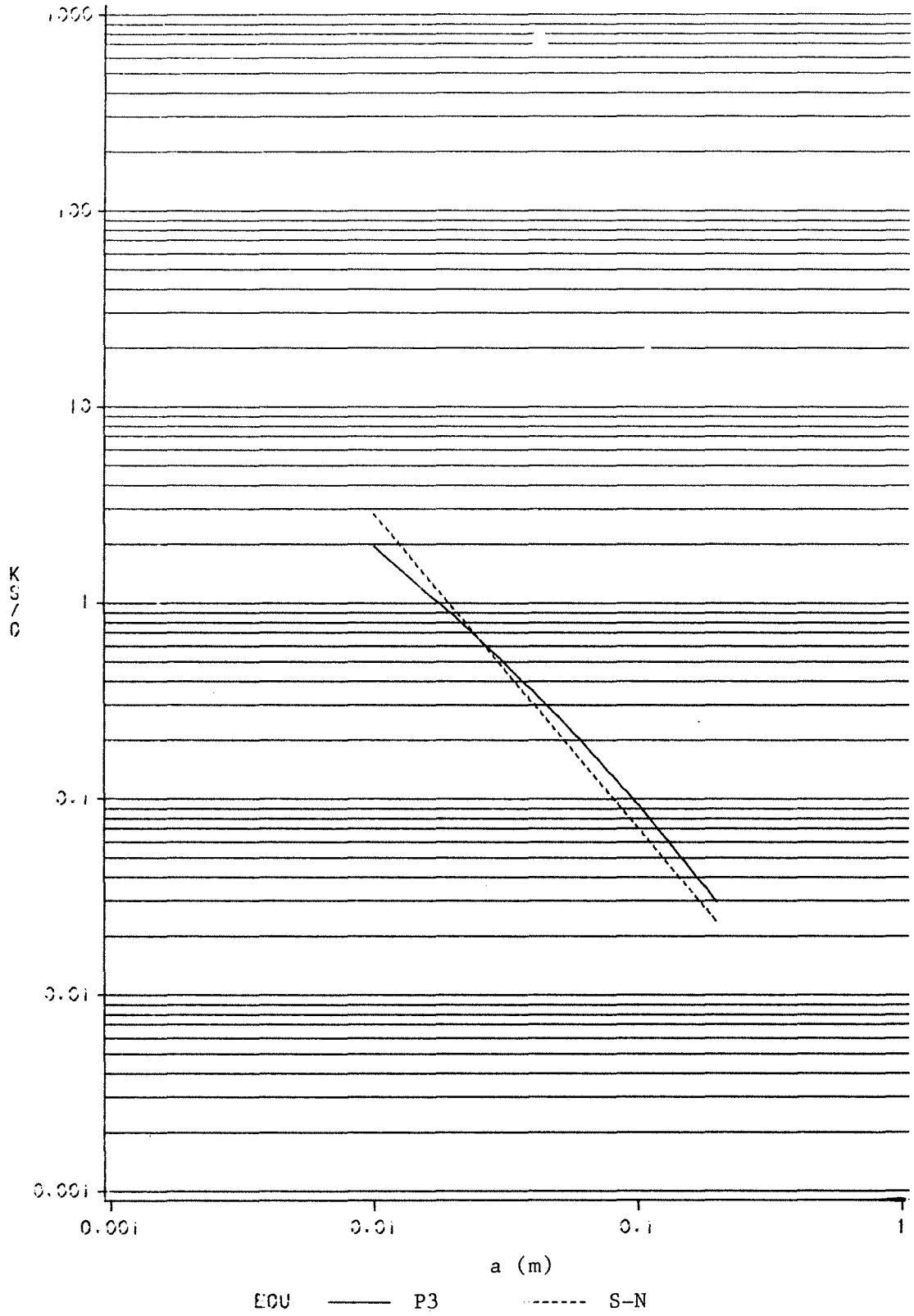

Figure 6 Variation of P3 and S-N solutions with a

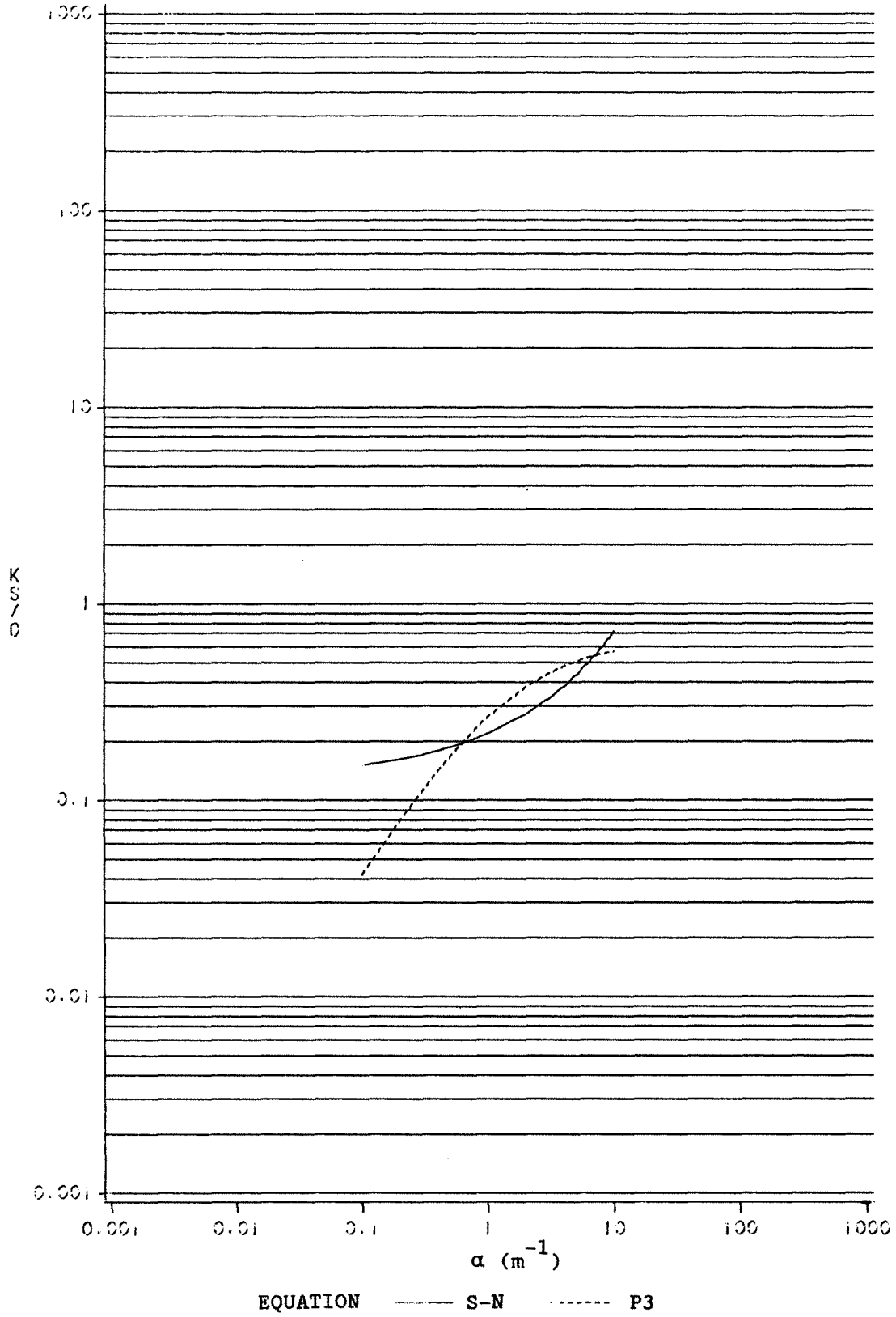

Figure 7 Variation of P3 and S-N solutions with α

4. Saturated-Unsaturated Unsteady Flow Models

One important practical consideration in the operation of the well permeameter is the time required to reach steady-state. According to Winger (1960), this time typically ranges between 2 and 6 days, whereas Talsma and Hallam (1980), with their design, claim that steady-state can be reached in 5 - 30 minutes. Saturated-unsaturated unsteady flow models can give information on the time required to reach steady-state, the factors which affect this time, and the volume of water required. In addition they can establish methods of estimating saturated hydraulic conductivity from early time data of a borehole infiltration test.

Stephens and Neuman (1982c) used the computer programs FLUMP and TRUST to carry out transient flow numerical experiments for a range of problems. In each case (unless otherwise stated) a borehole of 15 cm radius and a water column of 1 m depth were used. The initial and boundary conditions are described in their paper. Their results are summarised below.

4.1 Factors affecting infiltration rate

(a) Effect of soil type on infiltration rate

Numerical experiments were carried out on the four representative soils described previously. Several general observations were made:

- the infiltration rate was fastest in silt loam and fine sand, and slower in light clay and coarse sand. The same results were obtained under steady-state conditions and was attributed to differences in the water retention characteristics of the four soils. The behaviour of coarse sand was possibly linked to a numerical error.

- The saturated region around the borehole reached a constant size and shape after about 1.2 days but the flow rate did not become constant for 10 days after the start of the test. The wetting front, defined as the region of steepest water content gradient, continued to expand beyond its position of 10 days and reached a quasi-steady configuration some

time later. Thus steady-state in the saturated zone near the borehole was reached much earlier than in the unsaturated zone, and the flow rate stabilised after the establishment of steady-state in the saturated region.

(b) Effect of initial water content on infiltration rate

Numerical experiments were conducted for three different uniform initial volumetric water contents of 60%, 78% and 93% saturation. The results showed that infiltration rate decreased with increasing antecedent water content due to the corresponding reduction in hydraulic gradients. This effect was much more pronounced at the early stages of the test than at later times. At steady-state, the effect of background water content on flow rate under deep water table conditions was shown to be minor.

(c) Effect of anisotropy on infiltration rate

The effect of anisotropy on infiltration rate was tested for the silt loam with a horizontal saturated conductivity, K_h, of 0.5 m d^{-1} and a vertical saturated conductivity, K_v, of 0.05 m d^{-1}. At early time most of the flow was found to take place in response to horizontal hydraulic gradients normal to the length of the borehole, and the infiltration rate was controlled by K_h. As time progressed, gravity exerted increasing influence on the flow pattern and the effect of K_v became increasingly important. At steady-state the infiltration rate in this soil was 56% of the rate in a similar isotropic soil with $K_v = K_h = 0.5$ m d^{-1}.

(d) Effect of borehole geometry on infiltration rate

The effect of borehole geometry on infiltration rate was investigated for the silt loam and the results are shown in Fig. 8. The results show that infiltration rate decreases as H, a and A (length of borehole in contact with soil) decrease, and the effect is much more pronounced at early time than at steady-state. The decrease in flow rate can be attributed to the decreased contact area between the soil and the borehole, as a and A decrease, and to the decrease in head as H decreases.

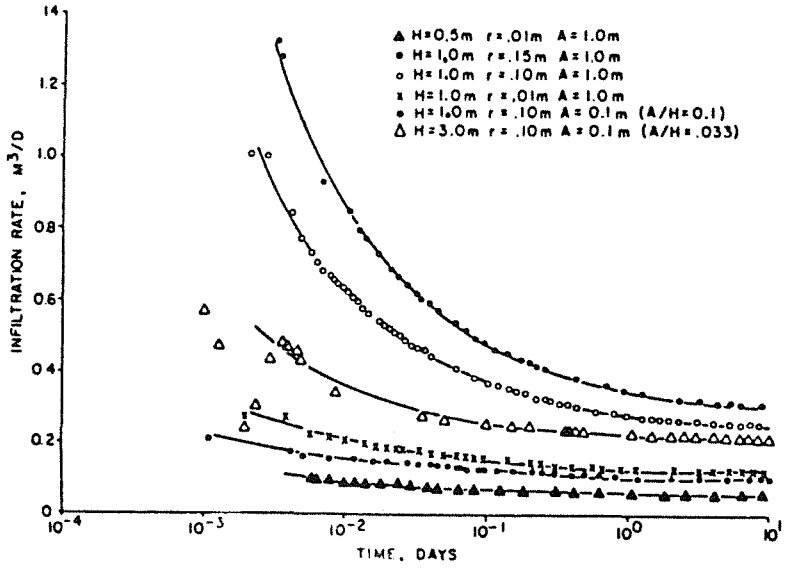

Figure 8 Infiltration rate as a function of time in GE3 silt loam for different bore hole geometries (here r = borehole radius, A = length of borehole in contact with soil) (from Stephens & Neuman, 1982c)

4.2 Time required to reach a steady infiltration rate

Estimates of the time required to reach a steady infiltration rate (Q_s) range from 5 minutes (Talsma and Hallam, 1980) to 6 days (Winger, 1960). This question was investigated by Stephens and Neuman (1982c) who considered the effects of soil texture, antecedent water content, saturated hydraulic conductivity, anisotropy, and borehole geometry.

For the set-up with a borehole radius of 15 cm, a head of water of 1 m, a background vertical flow rate of 1.5×10^{-3} m d^{-1} and an assumed saturated hydraulic conductivity of 0.05 m d^{-1} for each of the four test soil types, the time required to reach 95% of Q_s ranged from 4 - 8 days. To reach 80% of Q_s required 10-17 hours, with silt loam the fastest and fine sand the slowest.

Increasing the antecedent water content had the effect of decreasing the time to reach Q_s. For the silt loam with the above conditions, the time required at 93% saturation to reach 80% of Q_s was 3 hours, while at 60% saturation, it was 16 hours. To reach 90% of Q_s the respective times were 9 hours and greater than 2 days.

Model simulations to test the effect of anisotropy in saturated hydraulic conductivity showed that the time to reach Q_s is governed principally by the vertical conductivity.

Variation of the saturated hydraulic conductivity K_s (other variables remaining constant) showed that increasing K_s by a factor of 10 decreased the time to reach any given value of Q_s/Q by exactly the same factor.

Conversely, decreasing K_s by a factor of 10 increased the time by the same factor. Thus in low permeability soils several weeks or months may be required to reach a steady infiltration rate.

The effects of borehole geometry on the time to reach Q_s are shown in Fig. 9. Reducing borehole radius from 15 cm to 1 cm (keeping other variables constant) was found to reduce the time to reach 90% of Q_s by about 50%. Decreasing the head of water from 1 m to 50 cm, with a = 1 cm, reduced the time to reach 90% of Q_s by about 40%. Thus to minimise the measurement time of the uncased borehole permeameter would require minimising the borehole radius and the constant head of water. Both of these requirements effectively reduce the soil/water contact area in the borehole.

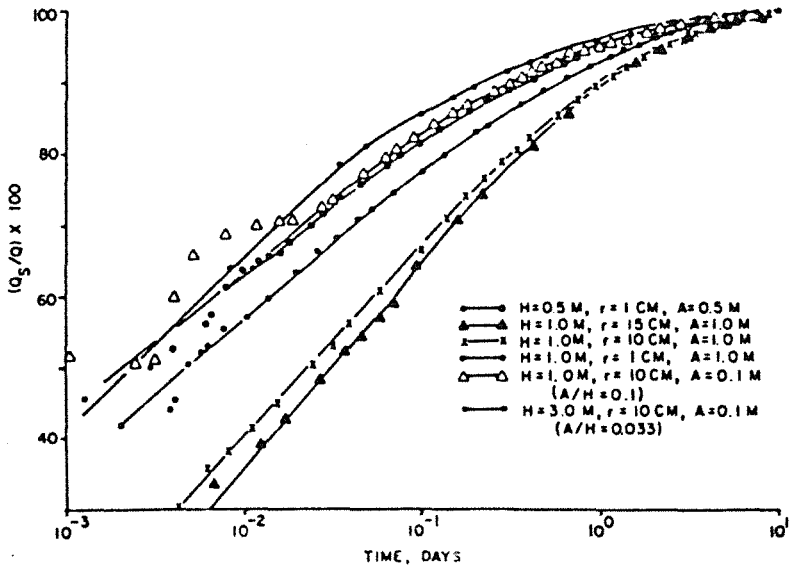

Figure 9 Percentage of steady infiltration rate as function of time for different borehole geometries in GE3 silt loam (here r = borehole radius, A = length of borehole in contact with soil) (from Stephens and Neuman, 1982c)

4.3 Volume of water required per measurement

The inflow volumes of water required under saturated-unsaturated conditions to reach 80%, 90% and 95% of Q_s in the four representative soils were numerically computed using FLUMP by Stephens and Neuman (1982c) and are listed in Table 5. The soil moisture deficit, $\Delta\Theta$, was defined as the difference between water content at saturation and average initial water content near the borehole. Specific yield, S_y, was estimated from the soil water characteristics of each soil. It is clear from the results that the volume of water required is most sensitive to borehole geometry and that volumes can be minimised by using small diameter boreholes. The volume is also seen to be sensitive to initial percentage saturation, decreasing significantly as percentage saturation increases.

Table 5 Volumes of water required to reach steady infiltration rates

Soil Type	H (m)	γ	K_s (md^{-1})	S_y	$\Delta\Theta$	Volume inflow to reach given % of Q_s 80% (L)	90% (L)	95% (L)
silt loam	0.5	50	0.05	0.08	0.087	7.3	50	148
	1.0	100	0.05	0.08	0.087	23.4	87	220
	1.0	10	0.05	0.08	0.087	140	370	715
	1.0	6.67	0.05	0.08	0.087	156	346	485
	1.0	6.67	0.5	0.08	0.087	179	460	-
		6.67	K_h= 0.5 K_v= 0.05	0.08	0.087	620	2740	7760
	1.0	6.67	0.05	0.08	0.157	340	785	1600
	1.0	6.67	0.05	0.08	0.027	65	130	240
light clay	1.0	6.67	0.05	0.21	0.166	189	412	770
fine sand	1.0	6.67	0.05	0.26	0.225	330	685	1150
coarse sand	1.0	6.67	0.05	0.29	0.199	134	309	498

The authors found that the USBR (1974) formulae for determining water volume requirements significantly underestimated their numerically determined values, with USBR maximum volume estimates ranging from 12%-99% of the numerically determined volumes necessary to reach 95% of Q_s. The authors were not able to develop a general method of estimating water volume requirements but found that, for isotropic soils, the volumes required to reach 0.9 Q_s were 2-3 times greater than that needed to reach 0.8 Q_s, and the volumes required to reach 0.95 Q_s, were 4-6 times greater than that needed to reach 0.8 Q_s.

4.4 Determining saturated hydraulic conductivity from early time data

All the formulae to compute saturated hydraulic conductivity (K_s) described in previous sections require a value for Q_s. However, as highlighted in section 4.2, it may take several hours, days or weeks for steady infiltration rates to be obtained. Based on the transient numerical experiments, the authors identified two methods of obtaining K_s from early time measurements for isotropic soils.

The first method involves plotting inverse flow rate (Q^{-1}) against the logarithm of time. According to the numerical results, the plotted data follow a straight line up to when $Q = 0.8\ Q_s$, at which point there is a change in slope. Thus the break in slope can be used to estimate Q_s and, once the break is identified, measurements can be terminated.

The second method is to plot Q against $t^{-1/2}$. Analytical solutions for 1-dimensional infiltration into soils of uniform initial water content by Green and Ampt (1911) and Philip (1969) showed that, when the applied head is constant, Q is approximately proportional to $t^{-1/2}$. Plotting the numerical results of Stephens and Neuman (1982c) in the same way showed that the silt loam and light clay lied on well-defined straight lines. The fine and coarse sands showed curvature at early time but fell on a straight line at later time. Extrapolating the straight line segments to infinity (i.e. $t^{-1/2}=0$) gives Q_s. Once the straight line segment has been observed, field measurements can be terminated.

5. Concluding Discussion

5.1 General

A considerable number of analytical and numerical analyses of the constant head well permeameter have been carried out. Many of these date back in excess of 25 years but several more sophisticated numerical and analytical studies have been reported recently. Some of the more significant analyses have been reviewed in this report. In all cases a number of simplifying assumptions have been made which could affect the validity of the prediction of saturated hydraulic conductivity in field conditions. The assumptions are:

(a) no account is taken of soil heterogeneity
(b) no account is taken of macropore flow
(c) no account is taken of air entrapment
(d) in most of the analyses, no account is taken of anisotropy
(e) in all but two of the most recent analyses, no account is taken of flow in mixed saturated-unsaturated conditions.

In respect of the effect of air entrapment, it is generally recognised that the well permeameter does not measure a completely saturated hydraulic conductivity but rather a lower 'field-saturated' conductivity. Some authors have reported a conductivity reduction of as much as 50% below the completely saturated value (Bouwer and Jackson, 1974). However the field-saturated conductivity measured by the well permeameter may be more representative of both natural and man-made infiltration processes.

5.2 Saturated flow analyses

All the analyses are based on the assumption that the flow region is fully saturated, and most of them treat the external boundary of this region as a free surface. The relative accuracy of the different analyses is dependent on the closeness to which the boundary conditions at the well surface and the boundary of the saturated region are satisfied, and on the accuracy of the approximation of the vertical and horizontal hydraulic pressure gradient distributions along the well surface. Comparison of the saturated flow formulae over a range of γ

revealed moderately good agreement with the exception of the least accurate Porchet solution. The bandwidth of solutions for K_s/Q decreased slightly with increasing γ, and the gradients became high at $\gamma<20$ indicating that small errors in γ could give large errors in K_s/Q.

5.3 Saturated-unsaturated flow analyses

Two analyses (Stephens and Neuman, 1982b; Philip, 1985a) have recently dealt with mixed saturated-unsaturated flow from an open well. The major conclusion from both analyses is that the predicted K_s/Q values are significantly less than for the assumption of saturated flow alone. This result is physically reasonable because the effect of capillarity is to provide an additional force moving water away from the well in addition to gravity and pressure. Thus to obtain the saturated hydraulic conductivity, the capillarity component effectively has to be subtracted from the field measured value.

The empirical numerically derived formula for K_s/Q of Stephens and Neuman (1982b) agrees fairly well with Philip (1985) over the normal range of γ, α and a. Because three variables are involved it is not straightforward to specify under which values of γ, α and a that the two analyses agree or disagree most. As with the saturated flow formulae, K_s/Q is more sensitive to γ at low γ. On a log-log scale K_s/Q v a is approximately linear for both solutions, implying that their predicted values will not vary greatly with 'a'. The gradient however is steep, indicating that small errors in 'a' may result in large errors in K_s/Q. As regards α, the log-log relationship for the two solutions are non-linear and of inverted curvature, such that exact agreement is obtained at intersecting points for given a, γ. The mean gradient of the curves is somewhat lower than for 'a', indicating that K_s/Q would have more tolerance to errors in α.

The effect of capillarity on the predicted K_s/Q values was found to be significantly stronger in the Philip (1985a) solution than the Stephens and Neuman (1982b) solution. In both cases capillarity effects were greater for finer soils. In the Philip (1985a) solution, the effect of capillarity was found to decrease with increasing H and a, but this was not the case with the Stephens and Neuman (1982b) solution.

The saturated-unsaturated unsteady flow model analyses of Stephens and Neuman (1982c) identified a number of important characteristics useful to the design and operation of the constant head well permeameter. Factors found to affect the infiltration rate were soil type, initial water content, anisotropy and borehole geometry. The time to reach steady state infiltration was affected by the same factors. Saturated hydraulic conductivity had the greatest effect, being inversely proportional to time to steady state. Increasing the antecedent water content, reducing the borehole radius, and decreasing the head of water, all decreased the time to reach a steady state infiltration rate. The volume of water required per measurement decreased with decreasing bore diameter and increasing antecedent water content.

In summary the most efficient constant head permeameter design would be one which minimised the water/soil contact area, i.e. one that required a small borehole diameter and head of water. Stephens and Neuman (1982c) also described two methods of determining saturated hydraulic conductivity from early time data, so that measurements can be terminated prior to steady state infiltration being reached. These methods require further field evaluation.

Acknowledgements

The author would like to thank Mr J.K. Ruprecht for carrying out some numerical computations and producing some graph plots.

References

Boersma, L. (1965). Field measurement of hydraulic conductivity above a water table. In : Methods of Soil Analysis (C.A. Black, ed.), Agronomy 9, 234-52, Am. Soc. Agron., Madison, Wis.

Bouwer, H. and Jackson, R.D. (1974). Determining soil properties. In : Drainage for Agriculture (J. van Schilfgaarde, ed.), Agronomy 17, 611-72, Am. Soc. Agron., Madison, Wis.

Carlsaw, H.S. and Jaeger, J.C. (1959). Conduction of heat in solids, 2nd ed., Clarendon, Oxford.

Glover, R.E. (1953). Flow from a test-hole located above ground-water level. In : Theory and Problems of Water Percolation, USBR Eng. Monograph No. 8, 69-71.

Green, H.A. and Ampt, G.A. (1911). Studies on soil physics. I. Flow of air and water through soils. J. Agric. Sci. 4, 1-24.

Mualem, Y. (1976). A catalog of the hydraulic properties of unsaturated soils. Research Project 442, Technion-Israel Institute of Technology, Haifa.

Narasimhan, T.N. and Witherspoon, P.A. (1977). Numerical model for saturated-unsaturated flow in deformable porous media, Part I :Theory. Water Resour. Res. 13 (3), 657-64.

Narasimhan, T.N., Neuman, S.P. and Witherspoon, P.A. (1978). Finite element method for subsurface hydrology using a mixed explicit-implicit scheme. Water Resour. Res. 14 (5), 863-77.

Nasberg, V.M. (1951). The problem of flow in an unsaturated soil for injection under pressure. Izvestja Akademia Nauk, SSSR Odt Tekh Nauk, No. 9.

Neuman, S.P. (1976). Users Guide for FREESURF I. Dept. of Hydrology and Water Resources, University of Arizona, Tucson, Ariz.

Neuman, S.P. and Witherspoon, P.A. (1970). Finite element method for analysing steady seepage with a free surface. Water Resour. Res. 6 (3), 689-97.

Neuman, S.P. and Narasimhan, T.N. (1977). Mixed explicit-implicit iterative finite element scheme for diffusion-type problems : 1. Theory. Internat. J. Numer. Methods in Eng. 11, 309-23.

Philip, J.R. (1966). Absorption and infiltration in two- and three-dimensional systems. In : Water in the Unsaturated Zone, Vol. 1 (R.E. Rijtema and H. Wassink eds.), UNESCO, Paris, 503-25.

Philip, J.R. (1969). Theory of Infiltration. Adv. Hydrosci. 5, 215-96.

Philip, J.R. (1985a). Approximate analysis of the borehole permeameter in unsaturated soil. Water Resour. Res. 21 (7), 1025-33.

Philip, J.R. (1985b). Steady absorption from spheriodal cavities. Soil Sci. Soc. Am. J. 49.

Reynolds, W.D., Elrick, D.E. and Topp, G.C. (1983). A reexamination of the constant head well permeameter method for measuring saturated hydraulic conductivity above the water table. Soil Sci. 136, 250-68.

Stephens, D.B. and Neuman, S.P. (1982a). Vadose zone permeability tests : summary. J. Hydraul. Div. Am. Soc. Civ. Eng. 108, 623-39.

Stephens, D.B. and Neuman, S.P. (1982b). Vadose zone permeability tests : steady state results. J. Hydraul. Div. Am. Soc. Civ. Eng. 108, 640-59.

Stephens, D.B. and Neuman, S.P. (1982c). Vadose zone permeability tests : unsteady flow. J. Hydraul. Div. Am. Soc. Civ. Eng. 108, 660-77.

Talsma, T. and Hallam, P.M. (1980). Hydraulic conductivity measurement of forest catchments. Aust. J. Soil Res. 30, 139-48.

Terletskaya, N.M. (1954). Determination of permeability in dry soils. Hydroelectr. Water Works 2.

USBR (1974). Earth Manual 2nd edn., USPO, Washington D.C.

USBR (1977). Ground Water Manual, USPO, Washington D.C.

Winger, R.J. (1960). In-place permeability tests and their use in subsurface drainage. Int. Comm. Irrig. Drainage, 4th Congr., Madrid, III, 417-69.

Zangar, C.N. (1953). Theory and problems of water percolation. USBR Eng. Monograph No. 8.

7754R